The Journal of Experimental Biology 213, 2536-2546

doi:10.1242/jeb.039792

Adrenergic control of swimbladder deflation in the zebrafish (*Danio rerio*)

Tristan C. Dumbarton[1], Matthew Stoyek[1], Roger P. Croll[1,*] and Frank M. Smith[2,*,†]

[1]Department of Physiology and Biophysics and [2]Department of Anatomy and Neurobiology, Dalhousie University, 5850 College Street, Halifax, NS, Canada, B3H 1X5

*These authors contributed equally to this work
†Author for correspondence (fsmith@dal.ca)

Accepted 6 April 2010

SUMMARY

Many teleosts actively regulate buoyancy by adjusting gas volume in the swimbladder. In physostomous fishes such as the zebrafish, a connection is maintained between the swimbladder and the oesophagus *via* the pneumatic duct for the inflation and deflation of this organ. Here we investigated the role of adrenergic stimulation of swimbladder wall musculature in deflation of the swimbladder. Noradrenaline (NA), the sympathetic neurotransmitter (dosage 10^{-6} to 10^{-5} mol l^{-1}), doubled the force of smooth muscle contraction in isolated tissue rings from the anterior chamber, caused a doubling of pressure in this chamber *in situ*, and evoked gas expulsion through the pneumatic duct, deflating the swimbladder to approximately 85% of the pre-NA volume. These effects were mediated by β-adrenergic receptors, representing a novel role for these receptors in vertebrates. No effects of adrenergic stimulation were detected in the posterior chamber. In a detailed examination of the musculature and innervation of the swimbladder to determine the anatomical substrate for these functional results, we found that the anterior chamber contained an extensive ventral band of smooth muscle with fibres organized into putative motor units, richly innervated by tyrosine hydroxylase-positive axons. Additionally, a novel arrangement of folds in the lumenal connective tissue in the wall of the anterior chamber was described that may permit small changes in muscle length to cause large changes in effective wall distensibility and hence chamber volume. Taken together, these data strongly suggest that deflation of the zebrafish swimbladder occurs primarily by β-adrenergically mediated contraction of smooth muscle in the anterior chamber and is under the control of the sympathetic limb of the autonomic nervous system.

Key words: buoyancy, sympathetic nervous system, immunohistochemistry, force of contraction, autonomic nervous system, innervation, anatomy, smooth muscle physiology.

INTRODUCTION

Approximately half of the extant teleosts use a gas-filled organ, the swimbladder, to generate lift to counteract the force of gravity on dense body tissues. The gas volume in this organ is adjustable so that these animals can attain neutral buoyancy at a given depth, presumably allowing a significant reduction in the energetic cost of locomotion-generated lift that would otherwise be required to maintain vertical position in the water column (Denton, 1961; Scheid et al., 1990; Alexander, 1993; Pelster, 1997; Webber et al., 2000; Pelster, 2009). Physostomous fish maintain into adulthood a patent connection, the pneumatic duct, between the swimbladder and the oesophagus, and can inflate or deflate the swimbladder by passing gas through this duct. Most of these fish can also transfer gas between the swimbladder and the blood stream by physiological mechanisms of secretion and resorption similar to those used by physoclistous fish, which do not have a patent pneumatic duct as adults (Fange, 1983; Alexander, 1993). However, some physostomes lack these physiological mechanisms or have very inefficient and slow gas transfer to or from the bloodstream, so these fish must depend primarily upon the passage of gas through the pneumatic duct to alter swimbladder volume and thus regulate buoyancy.

The basic physiological mechanisms for adjusting swimbladder volume are known for both physostomous and physoclistous fishes (for reviews, see Harden-Jones and Marshall, 1953; Alexander, 1966; Fange, 1966; Fange, 1983; Alexander, 1993), but few studies to date have addressed neural control of this function. The pre-eminent role of the autonomic nervous system, acting through short-latency inflation and deflation reflexes that target effectors within the swimbladder system, has been recognized (Nilsson, 1971; Nilsson, 1972; Campbell and McLean, 1994; Nilsson, 2009; Pelster, 2009) but the specific mechanisms of integrated reflex control of swimbladder volume are not understood for any teleost.

We therefore examined the mechanism of swimbladder deflation and its neural control in the zebrafish, a small fresh-water cyprinid native to shallow streams and ponds in Asia (McClure et al., 2006), as a potentially representative model for swimbladder function in this large group of fishes. This species has recently received widespread attention as a general vertebrate model for studying fundamental questions of organ function, development, behaviour and gene expression (Briggs, 2002; Miklósi and Andrew, 2006). The swimbladder in the adult zebrafish is located in the coelomic cavity, ventral to the vertebral column and dorsal to the gut. The anterior and posterior chambers are connected by a constriction, the communicating duct, while the pneumatic duct connects the posterior chamber to the oesophagus. Our laboratory has recently described the general anatomy of the zebrafish swimbladder, along with a detailed analysis of the organization of the musculature, vasculature and innervation of the posterior chamber (Finney et al., 2006). Gas enters or leaves the swimbladder *via* the pneumatic duct and we proposed that contractions of the lateral muscle bands in the posterior chamber would aid in deflation. That study also showed the presence of smooth muscle in the ventral portion of the anterior chamber, and we proposed that this musculature could play a role in resetting wall tension, and thus resonant frequency, to maintain

the acoustic properties of the swimbladder as the animal changed depth. In the present study we investigated the functional capability of the zebrafish swimbladder to actively adjust gas volume.

In the zebrafish the major autonomic innervation of the musculature in the posterior chamber appeared to be adrenergic, while the anterior chamber exhibited relatively less dense adrenergic terminal distribution (Finney et al., 2006). Here we hypothesize that the sympathetic nervous system mediates reflex control of swimbladder deflation, *via* adrenergic nerve terminals targeting smooth muscle in the posterior chamber. The first aim of the present study was thus to investigate the effects of the autonomic neurotransmitter noradrenaline (NA) applied exogenously to the swimbladder system. The results of these experiments showed that NA stimulated smooth muscle activity and promoted deflation primarily through actions on the anterior, not the posterior, chamber. We therefore examined the functional anatomy of the anterior chamber in detail to establish the organization of the musculature responsible for changes in volume, and the pattern of innervation of this musculature by putative sympathetic nerves.

MATERIALS AND METHODS

Zebrafish (*Danio rerio*, Hamilton 1822) were purchased from local suppliers (AquaCreations or PetsUnlimited, Halifax, NS, Canada) and were maintained in our laboratory facility using established procedures (Westerfield, 2007). All experiments were approved by the Dalhousie University Animal Care Committee and followed the animal use guidelines of the Canadian Council on Animal Care. Animals were maintained on a 14 h:10 h light:dark cycle in aquaria supplied with dechlorinated tap water at 28°C and were fed 2–3 times daily with Nutrafin flake fish food (Rolf C. Hagen Inc., Montreal, PQ, Canada) or live *Daphnia* sp. from a laboratory culture.

Volume, pressure and force measurement

For pharmacological experiments, zebrafish were rapidly anaesthetized in MS-222 (ethyl 3-aminobenzoate methanesulfonate salt; Sigma Chemical Co., Mississauga, ON, Canada; 0.02% w/v, pH 7.0) to minimize the possibility of catecholamine release into the circulation (Smit et al., 1979; Fabbri et al., 1998). Animals were exposed to anaesthetic for at least 3 min after opercular movement had ceased; this was found to be sufficient to kill the animals so that no supplementary anaesthetic was needed during experiments in which the swimbladder was investigated *in situ*. Animals were removed from the anaesthetic and pinned to the silicone rubber bottom of a small dish perfused with a saline solution (composition in mmol l^{-1}: NaCl, 130; $NaHCO_3$, 3.5; KCl, 5; KH_2PO_4, 1; $MgSO_4$, 1; $CaCl_2$, 1.5; glucose, 10) that was aerated with 5% CO_2/95% O_2 gas mixture; solution pH was 7.4. This perfusate solution was similar to that used by Nemtsas and colleagues for studying zebrafish cardiac tissue *in vitro* (Nemtsas et al., 2010). The coelom was opened ventrally to expose the swimbladder, which was cleared of the tunica externa and any adhering connective tissue. Throughout the dissection procedure and during experiments on the *in situ* swimbladder, this organ remained submerged, the heart continued beating, and care was taken to make sure blood flow through the retial vessels was maintained.

The effect of adrenergic stimulation on the volume of the entire swimbladder was recorded by photographing the lateral aspect of this organ before and during NA exposure. Effects on the volume of both chambers were then evaluated stereologically, using the procedure described by Robertson and colleagues (Robertson et al., 2008). Pressure inside the swimbladder chambers was measured *via* a 30 gauge needle inserted through the lateral chamber wall. Most preparations immediately formed a seal around the needle shaft so that no gas was lost and the existing intrachamber pressure was maintained. The needle was coupled *via* a water-filled length of polyethylene tubing (PE50, Clay Adams Co., Parsippany, NJ, USA) to a pressure transducer (Grass P23XL, Grass Technologies, West Warwick, RI, USA), the diaphragm of which was set at the same level as the midline of the fish. This level was less than 5 mm lower than the surface of the perfusate so any error in measured pressure caused by this difference was negligible. Pressure in the anterior chamber was measured after ligating the communicating duct with a fine thread; pressure in the posterior chamber was measured after ligating both the communicating duct and the pneumatic duct. The pressure transducer was calibrated using a 10 cm column of water.

To measure changes in force of contraction in isolated swimbladder tissue, 1 mm wide, circumferentially oriented rings of tissue were cut from the middle section of either the anterior or posterior chamber. One side of a ring was anchored to the bottom of the dish and the other side was attached to the beam of a force transducer (Grass FT-03,) mounted above the preparation on a manipulator. In preliminary experiments to determine whether the tissue ring preparation displayed a time-dependent visco-elastic relaxation that might have introduced errors into the tension measurements, we found that the tissue rings relaxed over a period of 10–20 min after slight pre-tensioning to remove the gross slack in the rings. A pre-tension force of 50 mN eliminated this component but did not affect the contractile responses to drug exposure. Therefore, prior to recording, all rings were pre-tensioned to a standard force of 50 mN. The transducer signal was amplified by a bridge amplifier (Grass 7P1) and recorded on videotape using a Vetter 3000A digital data recorder (Rebersburg, PA, USA). Selected segments of these recordings were then played back into an analog-to-digital converter (Axon Instruments 1322, Sunnyvale, CA, USA) and processed into digital files on a computer using AxoScope software (Axon Instruments). The force transducer was calibrated and its linearity checked by measuring beam deflections caused by known masses.

Gas was collected from the pneumatic duct in order to measure volume changes evoked by adrenergic stimulation of the whole swimbladder *in situ*. The pneumatic duct was resected near its junction with the oesophagus and the cut end was drawn gently into a fluid-filled glass pipette with a fire-polished tip sized to contain the duct. The pipette tip angled downward while the shaft was horizontal. Bubbles expelled from the swimbladder became lodged in the horizontal shaft. These bubbles were then photographed and their volume estimated by stereological morphometry similar to that for estimating whole swimbladder volume, using equations appropriate to the bubble shapes (Beyer, 1985). The accuracy of this estimation procedure was checked by injecting known volumes of air into the collection pipette from a graduated Hamilton microsyringe.

Drug application

All pharmacological agents used in this study were purchased from Sigma Chemical Co. Drug solutions were freshly made in saline solution on the day of each experiment. NA and isoproterenol, which are subject to rapid oxidation in solution, were prepared in saline solution containing 0.01% (w/v) ascorbic acid as an antioxidant (Sun and Ng, 1998). Solutions were applied to the preparation through a switching valve. In preliminary trials, drugs contacted the preparation within 30 s of switching perfusate flow and reached full concentration in an additional 30–60 s. Controls for drug effects were

performed by exposing tissue to vehicle alone for the same duration as in the experiments. Drugs applied to the preparation were: L-noradrenaline hydrochloride, phenlyephrine hydrochloride, phentolamine hydrochloride, isoproterenol hydrochloride, timolol maleate salt and atenolol.

Histochemistry and immunohistochemistry

Histochemistry and immunohistochemical labelling were used to identify musculature and innervation patterns in whole-mounts of the walls of the swimbladder, following protocols previously established in our laboratory (Finney et al., 2006). Briefly, whole swimbladders were removed after MS-222 anaesthesia and fixed in 4% (w/v) paraformaldehyde (TAAB, Aldermaston, Berks, UK) in phosphate-buffered saline (PBS: 0.1 mol l^{-1} Na_2HPO_4, 140 mmol l^{-1} NaCl; pH 7.2) for 2–4 h. Tissues were rinsed in PBS then placed in a PBS solution containing 1% (w/v) bovine serum albumin and 4% (v/v) Triton X-100 detergent, to block non-specific antibody binding and to permeabilize the tissue. For detailed examination of swimbladder musculature, tissues were incubated overnight with phalloidin (TRITC-conjugated phalloidin, 1:500 dilution in PBS, Sigma Chemical Co., *N*=12) to label F-actin (Small et al., 1999).

To demonstrate general innervation in the swimbladder walls, tissue was exposed to the monoclonal zn-12 antibody, a pan-neuronal axon marker in zebrafish (Trevarrow et al., 1990; Finney et al., 2006) obtained from the Developmental Studies Hybridoma Bank (Iowa City, IA, USA) and used at a dilution of 1:400 in PBS. Antibodies against tyrosine hydroxylase (TH), an enzyme in the synthesis pathway for NA and thus a presumptive marker for adrenergic innervation, were used to demonstrate potential sympathetic axons (Edwards and Michel, 2002; Finney et al., 2006). A mouse monoclonal antibody against TH (Immunostar, Hudson, WI, USA) was used at a dilution of 1:300 in PBS. Both antibody solutions also contained 0.05% Triton X-100 in PBS, and tissues were incubated for 5–7 days at 4°C with agitation. After exposure to primary antibodies, tissues were rinsed and incubated with secondary antibodies (anti-mouse Alexafluor 555, raised in goat; Invitrogen Canada Inc., Burlington, ON, Canada) at a dilution of 1:100 in PBS for 3 days in the dark. Negative controls for all antibodies used in this study were conducted by omitting the primary antibody from the above procedures.

Specimens were mounted in a solution of glycerol and Tris buffer (3:1, pH 8.0) containing 2% *n*-propyl gallate, an anti-fade agent (Giloh and Sedat, 1982), and examined using a Zeiss LSM 510 laser scanning confocal microscope (Carl Zeiss Ltd, Toronto, ON, Canada). *Z*-stacks of images from 20–50 optical slices spaced 0.2–2 μm apart were created, then compiled and processed using Zeiss Zen 2008LE software. Digital photomicrographs were assembled into plates using Adobe Photoshop 7 (Adobe Systems Inc., San Jose, CA, USA).

Statistical analysis

Data are presented as means ± 1 s.e.m. The level of significance for all statistical tests was set at $P \leq 0.05$. A Levene's test for homogeneity of variance was used to test the assumption of equal variance within datasets. Pairwise comparisons of means were performed using *t*-tests (paired or independent samples, as appropriate). For the gas collection experiments, trials with no drug application and trials with no concentration of agonist evoked no gas production; these cases were designated '0-yield' and one-sample *t*-tests were then used to statistically compare among all drug concentrations evoking non-0 yields with 0-yield data. All statistical procedures were performed using SPSS 15.0 (SPSS Inc., Chicago, IL, USA).

RESULTS

Responses to adrenergic stimulation

Effects on volume and pressure

The volume of the whole *in situ* swimbladder decreased upon application of NA. Photographs of the swimbladder taken before and after 10 min exposure to 10^{-5} mol l^{-1} NA (Fig. 1) showed an obvious change in the volume of the anterior but not the posterior chamber (Fig. 1B, arrows). Mean total volume of the swimbladder was 15.9±1.6 μl before NA application (*N*=7). This was reduced significantly to 13.9±1.9 μl after 10 min NA exposure (*N*=7). NA-driven changes in volume were accompanied by inverse changes in pressure when recorded from isolated swimbladders with ligatures on the ducts. Mean pre-NA internal pressure in the isolated anterior chamber was 0.88±0.17 kPa (*N*=5) and 0.49±0.13 kPa (*N*=4) in the isolated posterior chamber. A typical response of anterior chamber pressure to NA exposure (10^{-5} mol l^{-1}, at arrow) is shown in Fig. 1C; here pressure approximately doubled over the course of 10 min adrenergic stimulation. Mean pressure in the anterior chamber after NA exposure was 1.78±0.27 kPa (*N*=5), a significant increase of 102% over the pre-NA mean value. The same dose of NA had no effect on pressure in the isolated posterior chamber.

Effects on force of contraction in isolated tissue rings

Noradrenaline evoked the effects described above by directly activating smooth muscle in the swimbladder wall, as demonstrated by the increased contractile force in rings of tissue taken from the anterior but not the posterior chamber (Fig. 2). A sample recording of the response to NA (10^{-5} mol l^{-1}) of tissue from the anterior chamber is shown in Fig. 2B; this dose of NA evoked a maximal response in this and the other samples tested. Maximal responses were reached within approximately 1 min after initiating NA application. All tissue rings dissected from the anterior chamber (*N*=5) responded to NA with a significant increase in contractile force; the mean response is shown in Fig. 2C. In contrast, no tissue rings from the posterior chamber displayed detectable responses to NA at the maximal dose tested (Fig. 2C).

Effects on gas expulsion

The overall effect of adrenergic stimulation of smooth muscle in the intact swimbladder *in situ* was to expel gas from the pneumatic duct. Perfusion of the swimbladder with normal saline or saline containing 0.01% ascorbic acid had no effect, and nor did bath application of NA at a dose of 10^{-7} mol l^{-1}. However, gas was always expelled when the swimbladder was exposed to NA concentrations of 10^{-6} or 10^{-5} mol l^{-1}. The first bubble of gas entered the pneumatic duct approximately 1.5 min after either of these two doses of NA reached the preparation and expulsion continued in some cases for up to 0.5 h. Mean values of expelled volume were therefore calculated from the total volume collected in each experiment during 0.5 h of exposure to NA. When the communicating duct was ligated, preventing gas from leaving the anterior chamber, there was no gas expelled from the pneumatic duct in the presence of NA at concentrations up to 10^{-5} mol l^{-1}.

Fig. 3 summarizes the quantitative effects of NA as well as those of adrenergic agonists and antagonists on expulsion of gas from the swimbladder system. Gas volume collected after application of NA at a concentration of 10^{-7} mol l^{-1} was 0 (Fig. 3, open bar in NA group; *N*=5); this 0-yield value was used for comparison with effects of greater NA concentrations. Mean volumes of gas expelled during

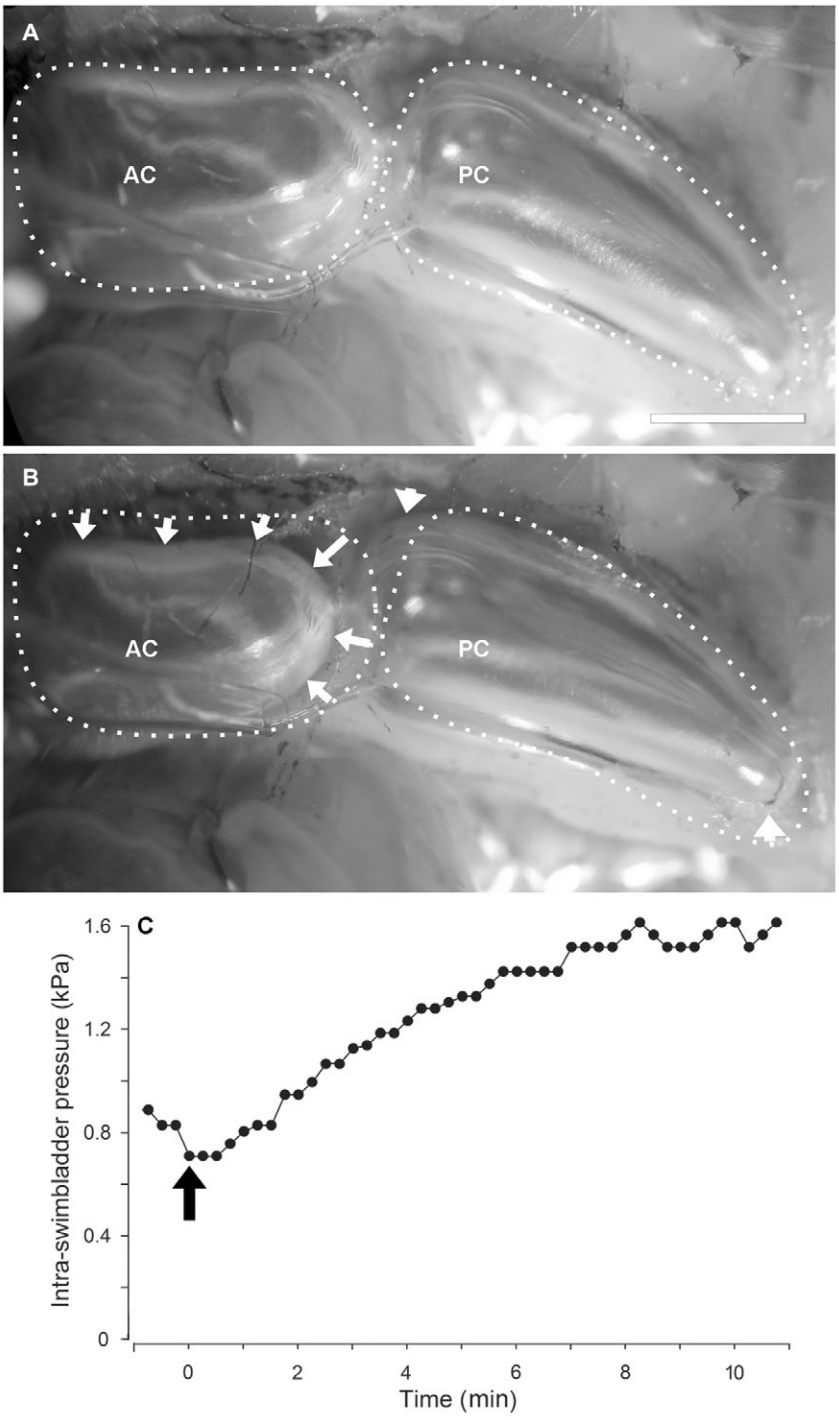

Fig. 1. Application of noradrenaline (NA) to swimbladder *in situ* evoked smooth muscle contractions in the anterior chamber that reduced volume and increased pressure. (A) Left lateral view of swimbladder before application of NA (control condition); in this and subsequent anatomical figures dorsal is upward and cranial to the left. The outlines of the anterior (AC) and posterior (PC) chambers are indicated by dotted lines. (B) Same specimen as in A, after exposure to NA (10^{-5} mol l^{-1}, 10 min in bath perfusate). Changes in the outline of the anterior chamber (to arrows) from the control outline (dotted line as in A) indicate that NA application decreased chamber volume. The posterior chamber shifted position (indicated by arrowheads) but did not change volume during NA exposure. The communicating duct was not ligated in these experiments. Scale bar: 1 mm in A and B. (C) In another specimen, NA (10^{-5} mol l^{-1}, bath-applied at arrow) increased pressure in the anterior chamber after ligation of the communicating duct.

exposure to NA concentrations of 10^{-6} mol l^{-1} (N=9) and 10^{-5} mol l^{-1} (N=7), as shown in Fig. 3 (hatched bars, NA group), were significantly greater than the control value (asterisks), but were not significantly different from each other. To determine the subtype of adrenergic receptor mediating this response, phentolamine (10^{-5} mol l^{-1}; N=5), a general α-adrenoreceptor antagonist, was co-applied with NA (10^{-5} mol l^{-1}). This produced a mean value of gas expulsion that was significantly greater than the control value but was not significantly different from the mean value for NA alone at a concentration of 10^{-5} mol l^{-1} (Fig. 3 black bar, +PT). However, co-application of either timolol (10^{-4} mol l^{-1}; N=6), a general β-adrenoreceptor antagonist, or atenolol (10^{-4} mol l^{-1}; N=6), a β_1-adrenoreceptor antagonist, with 10^{-5} mol l^{-1} NA eliminated the response (Fig. 3 black bars, +TI and +AT, respectively).

To confirm the potential involvement of β-adrenergic receptors in the response to NA, the swimbladder preparation was exposed to three concentrations of the general β-adrenergic receptor agonist isoproterenol in the perfusate (Fig. 3, ISO group of bars). A concentration of 10^{-7} mol l^{-1} isoproterenol caused no gas expulsion (open bar, N=5) so this was treated as the control for comparison with responses to higher concentrations of the agonist. Isoproterenol at concentrations of 10^{-6} mol l^{-1} (N=11) or 10^{-5} mol l^{-1} (N=7) evoked expulsion of gas volumes significantly greater than control; mean values of these gas volumes were in the same range as those evoked

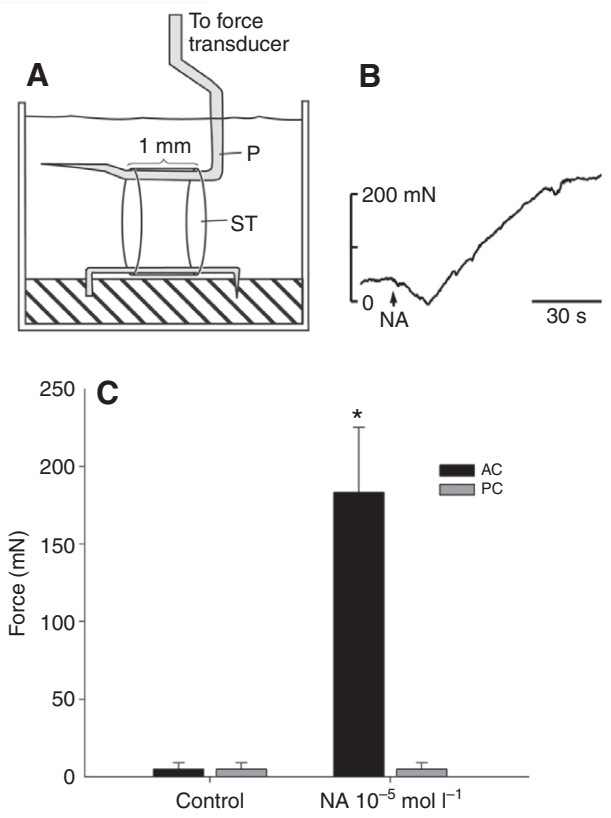

Fig. 2. Effects of NA on force of contraction of smooth muscle in rings of tissue cut transversely from swimbladder chamber walls. (A) Schematic diagram of *in vitro* preparation; tissue ring (ST) from the anterior or posterior chamber was anchored to the chamber bottom, coupled to a force transducer by a bent pin (P) and pre-tensioned to 50 mN for 5 min before NA application (see text). (B) Plot of the typical change in the force of contraction evoked by NA (10^{-5} mol l^{-1}, bath applied starting at the arrow). The transient initial decrease in force was an artifact due to switching bath flow. (C) NA caused a significant increase (asterisk) in the mean force of contraction in tissue from the anterior (black bars) but not posterior (grey bars) chamber.

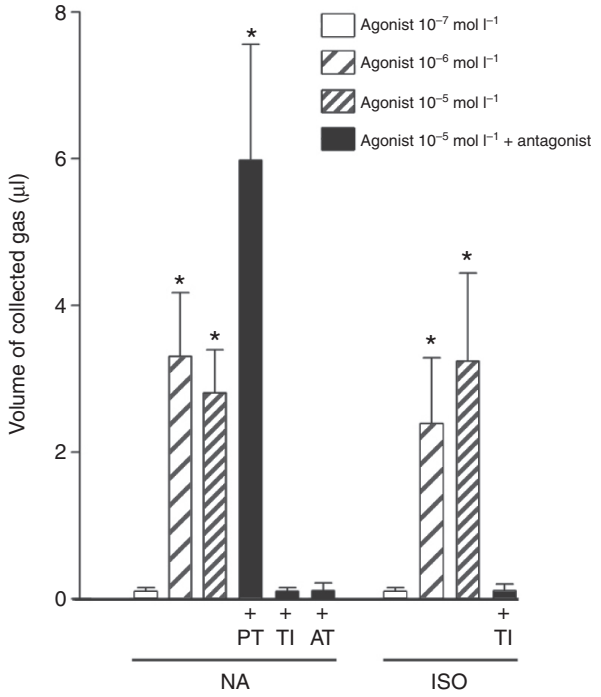

Fig. 3. Effects of bath-applied NA, adrenergic agonists and antagonists on expulsion of gas from the swimbladder *in situ*. Bars on the left side of the figure depict mean responses to NA. A dose of 10^{-7} mol l^{-1} NA (open bar) evoked no gas release (taken as 0-yield for statistical comparison) but greater NA doses (10^{-6} and 10^{-5} mol l^{-1}, hatched bars) caused significant release of gas volumes (asterisks). Phentolamine co-applied with NA (both 10^{-5} mol l^{-1}, solid bar, +PT) caused the release of a volume of gas significantly greater than control (asterisk) but not significantly different from that evoked by 10^{-5} mol l^{-1} NA alone. Timolol (10^{-4} mol l^{-1}, +TI) or atenolol (10^{-4} mol l^{-1}, +AT) co-applied with NA eliminated responses to this agonist. Bars on right side of the figure show responses to bath application of isoproterenol (ISO). A dose of 10^{-7} mol l^{-1} ISO (open bar) caused no gas release (taken as control) but higher concentrations (10^{-6} and 10^{-5} mol l^{-1}, hatched bars) evoked the release of gas volumes significantly greater than the control response (asterisks). There was no statistical difference between responses to 10^{-6} and 10^{-5} mol l^{-1} ISO. The response to 10^{-5} mol l^{-1} ISO was eliminated by co-application of timolol (10^{-4} mol l^{-1}, +TI).

by equivalent concentrations of NA (Fig. 3, NA group). Co-application of timolol (10^{-4} mol l^{-1}) with isoproterenol (10^{-5} mol l^{-1}; N=8) eliminated the response to the β-agonist (Fig. 3, +TI bar in ISO group).

Anatomy and innervation of the swimbladder musculature

Wall structure

The results of the functional studies above indicated that the anterior chamber, rather than the posterior chamber, appears to play the main role in swimbladder deflation. While the anatomy and innervation of the posterior chamber have been described previously (Finney et al., 2006), the detailed wall structure of the anterior chamber has not been determined. Here we examined the pattern of organization of the musculature in this chamber, by confocal imaging of phalloidin-labelled smooth muscle in whole-mount wall segments (Figs 4 and 5) and by darkfield microscopy of the intact organ (Fig. 6).

Muscular organization

The majority of myocytes in the anterior chamber were oriented circumferentially, forming a prominent ventral band (Fig. 4A,B and schematic diagram). Many myocytes in this region were grouped into what appeared to be bundles of approximately 40–50 fibres (Fig. 4A, brackets) which were gathered together near the lateral edge of the muscle band and fanned out as they coursed ventrally. Near the communicating duct, myocytes were present in a continuous distribution around the ostium of the duct (Fig. 4, schematic diagram). Fig. 4C shows that in this region most of the myocytes were also oriented circumferentially, with some radially oriented myocytes interwoven among the circumferential fibres. In the posterior chamber, sampled for comparison with the anterior chamber, smooth muscle fibres were present in bilateral bands along the full length of the chamber with fibres oriented mainly in the circumferential direction (data not shown, but see below). This pattern confirms a previous report of the structure of the wall in this chamber (Finney et al., 2006).

In addition to the pattern of musculature described above, there was a pattern of regularly spaced folds in the connective tissue underlying the muscle layer and adjacent to the lumen in the cranioventral and lateral aspects of the anterior chamber. These folds

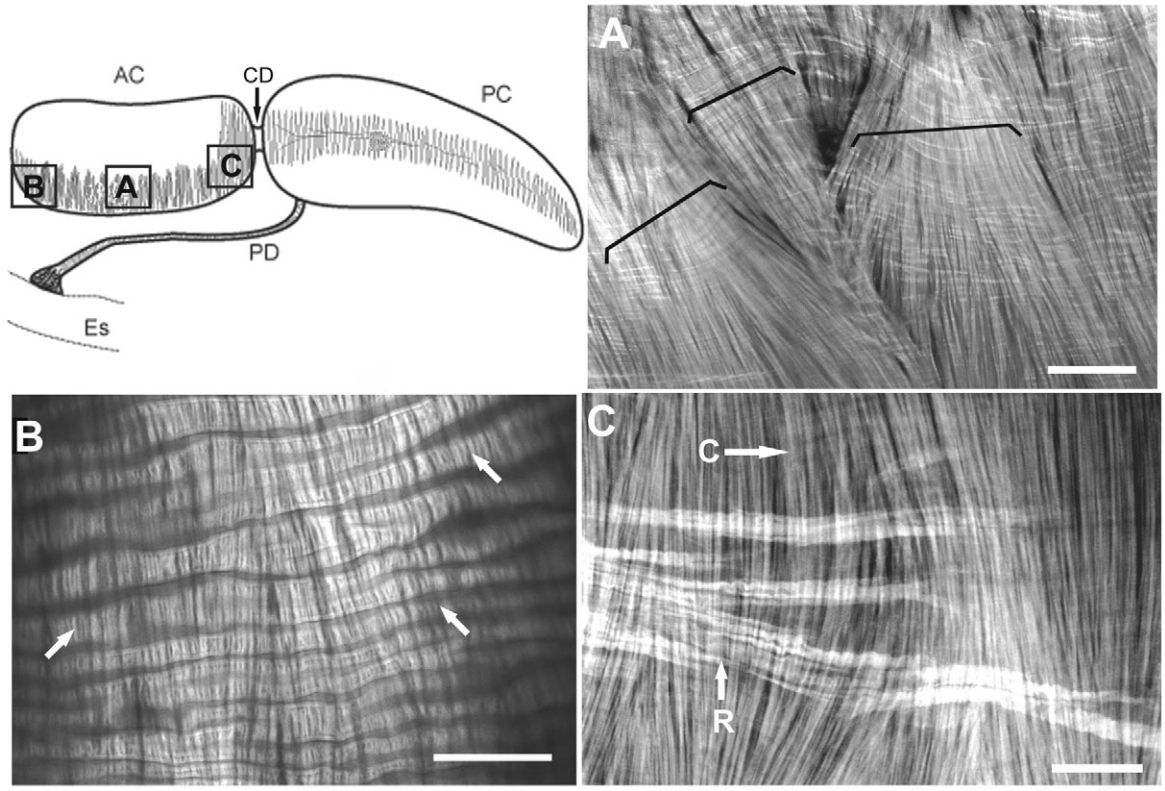

Fig. 4. Confocal imaging of F-actin labelled with phalloidin shows smooth muscle organization in the anterior chamber (AC). Shaded portions in the schematic diagram indicate muscular regions and A–C identify locations of photomicrographs in the corresponding panels. CD, communicating duct; Es, oesophagus; PC, posterior chamber; PD, pneumatic duct. (A) The majority of muscle fibres in the ventral band were oriented circumferentially and were frequently bundled into overlapping fascicles (brackets). (B) Connective tissue on the lumenal side of circumferential muscle fibres was thrown into regular folds (arrows) oriented along the anterior–posterior axis of the chamber and orthogonal to the main orientation of the muscle fibres. (C) Near the communicating duct, circumferential fibres (C) were interwoven with radial fibres (R). Scale bars: 50 μm in all photomicrographs.

can be seen in Fig. 4B (arrows). The direction of these folds was parallel to the long axis of the anterior chamber and therefore oriented orthogonally to the main orientation of the muscle fibres.

Details of the three-dimensional organization of folds in the walls of both chambers are visible in reconstructions made from stacks of confocal images taken with the *Z*-axis orthogonal to the lumenal surface, as shown in Fig. 5. In the ventral region of the anterior chamber, prominent folding is visible proximal to the lumenal surface (Fig. 5A), with layers of circumferential smooth muscle located external to the folded region. In comparison, the muscular layer in the posterior chamber wall in the region of the lateral muscle band was approximately four times as thick (Fig. 5B) as that in the ventral anterior chamber, but there was only a faint and relatively irregular pattern of folding of the connective tissue adjacent to the lumenal surface in the posterior chamber. These folds were, however, also oriented parallel to the long axis of this chamber.

In order to evaluate whether adrenergic stimulation of smooth muscle activity affected the folding in the ventral region of the anterior chamber, we observed this region in an *in vitro* preparation of the swimbladder using darkfield illumination, before and during NA exposure. A typical example is shown in Fig. 6. The folds were highly reflective with an interfold spacing of approximately 10 μm, but were only faintly visible before NA application (Fig. 6A,B). After 10 min exposure to NA (10^{-5} mol l^{-1}) in the perfusate bathing the swimbladder, the number of visible folds increased and their reflectivity was emphasized (Fig. 6C,D). There was also a significant decrease in the interfold distance of approximately one-third during NA exposure, from 11±0.2 μm pre-NA to 7±0.3 μm with NA (N=9; t-test).

Innervation

Anterior chamber

General innervation. Labelling with the general zebrafish neuronal marker zn-12 (N=15) showed widespread innervation of the anterior chamber (Fig. 7A). The small fibres comprising this innervation pattern appeared to ramify from several large nerve trunks (arrows, Fig. 7A) coursing into the anterior chamber *via* the wall of the communicating duct.

TH-like immunoreactivity. Fibres displaying TH-positive staining made up a subset of those demonstrated by zn-12 immunoreactivity. Comparison of images sampled from the dorsal and ventral regions of the same swimbladders (N=12) showed consistently that TH-positive fibres were more abundant in the ventral region (Fig. 7B) than in the dorsal region (Fig. 7C). Furthermore, in the cranioventral aspect of this chamber the area of greatest intensity of TH label overlapped with the region of thickest musculature (Fig. 7D, dashed line). TH-like immunoreactive fibres in the anterior chamber appeared to originate mainly from a single nerve traversing the communicating duct from the cranial aspect of the posterior chamber, although a minor contribution from a nerve accompanying a small blood vessel supplying the craniodorsal aspect of the anterior chamber was present in a few specimens (data not shown).

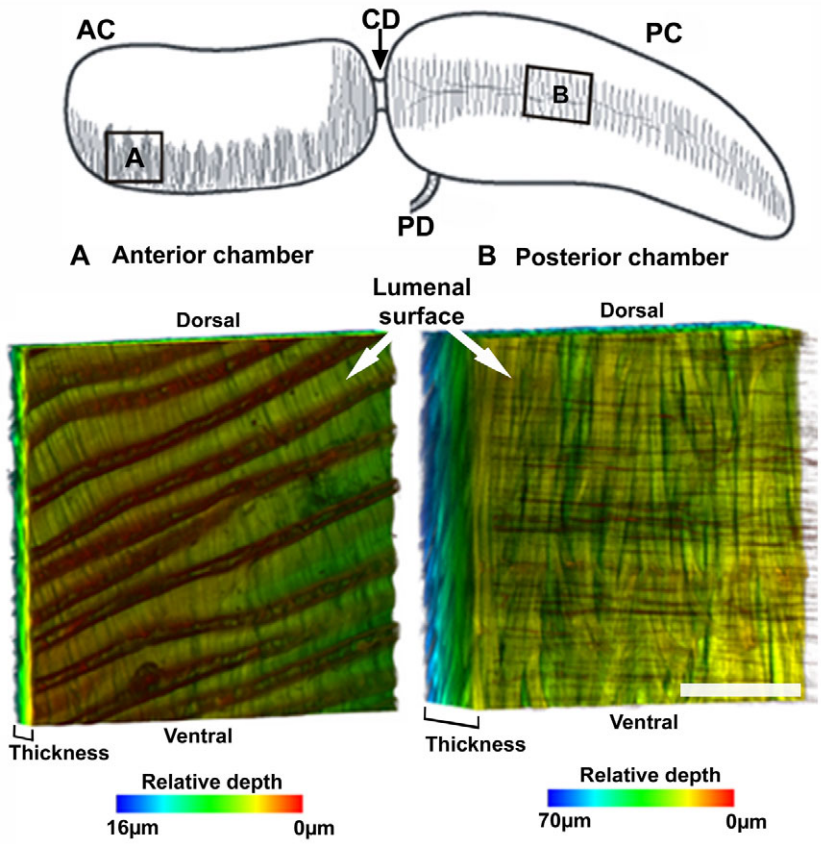

Fig. 5. Three-dimensional reconstruction of wall structure in tissue blocks from muscular regions of anterior (AC, panel A) and posterior (PC, panel B) chambers in areas indicated in the schematic diagram. Perspective images of tissue blocks were made from *Z*-stacks of confocal slices taken with the imaging plane parallel to the lumen; views are from the lumenal face (white arrows). (A) Appearance of folding in connective tissue adjacent to the lumen (contrasting horizontal bands); smooth muscle fibres appear in the tissue block as vertical striations deep to folds. In perspective, the relative thickness of the tissue block is indicated by the bracket in the lower left of the panel. The false-colour scale under the panel indicates relative depth from the lumenal surface of structures within the reconstructed tissue block through the entire thickness of the wall: red is proximal to the lumen, blue is toward the external surface (the length of these scales is exaggerated to show the colour gradations clearly). The overall thickness of the wall was 16 µm (note the length of the bracket at the lower left and the dimension on the false-colour scale bar). (B) Connective tissue folds were less evident in the posterior chamber wall than in the anterior chamber, while overall thickness of the lateral muscle band in the posterior chamber was 70 µm (note the length of the bracket and dimension on the false-colour scale bar relative to those in panel A). Scale bar within panel B represents 40 µm on the lumenal face in both panels.

Posterior chamber

TH-like immunoreactivity. The pattern of TH-positive innervation of the posterior chamber (*N*=12) was similar to that previously reported by Finney and colleagues (Finney et al., 2006), largely targeting the vasculature and muscles associated with the lateral muscle bands (Fig. 7E,F). Within the muscle bands there was a consistent pattern of nerve trunks containing numerous fibres coursing roughly in parallel with the long axis of the chamber, ramifying into single fibres projecting ventrally and dorsally to form extensive plexi within the muscle bands (Fig. 7E). The nerve trunks in this region arose as branches from TH-positive nerves accompanying the swimbladder artery; this feature of swimbladder innervation has not previously been reported. There was a high intensity of TH labelling associated with blood vessels of the posterior chamber, particularly of the rete mirabile (Fig. 7F), where punctate fluorescence indicated that putative varicosities were closely approximated to retial vessels.

DISCUSSION

We have shown that smooth muscle in the anterior chamber of the zebrafish swimbladder contracts, *via* activation of β-adrenergic receptors, to expel gas from the pneumatic duct. Given the circumferential orientation of most of the muscle fibres in this chamber wall, and the widespread adrenergic innervation of this musculature, we propose that deflation of the anterior chamber is under the control of the sympathetic limb of the autonomic nervous system. This mechanism therefore represents a key component of the reflex control of swimbladder volume in regulating buoyancy in this species.

Adrenergic control of swimbladder function

Our data support the hypothesis that swimbladder deflation results from the stimulation of adrenergic receptors on smooth muscle of the anterior chamber and the contraction of this muscle. The results of this study thus support the general concept that the sympathetic nervous system is involved in deflating the teleost swimbladder (Fange, 1983; Nilsson, 1983; Campbell and McLean, 1994; Nilsson, 2009). However, previous studies of the control of deflation have focused on the mechanism of resorption of gas from the swimbladder into the bloodstream in physoclists (which possess no pneumatic duct) and in a few physostomes. The proposed roles of the sympathetic nervous system were to reduce blood flow to the gas gland by vasoconstriction (chiefly by activating α-adrenergic receptors), and to relax smooth muscle in the swimbladder mucosa to increase the exposure of the resorptive epithelium to gas (activation of β-adrenergic receptors). In the present study we have found that deflation of the zebrafish swimbladder operates primarily by β-adrenoreceptor-mediated contraction of the smooth muscle in the wall of the anterior chamber to expel gas.

Three lines of evidence support this conclusion. First, NA consistently and directly promoted smooth muscle contraction in extirpated rings of tissue from the anterior but not the posterior chamber. Second, pressure measurements in isolated chambers showed that exogenously applied NA evoked increased pressure in the anterior but not the posterior chamber. Third, application of both NA and the β-adrenoreceptor agonist isoproterenol caused dose-dependent contractions of the anterior but not the posterior chamber, leading to expulsion of gas from the pneumatic duct. Pharmacological blockade of the α-adrenergic effects of NA did not significantly affect the swimbladder. Taken together these results strongly suggest that endogenous NA, released from sympathetic nerve terminals onto smooth muscles in the anterior chamber, would cause these muscles to contract, forcing gas out of this chamber. The ultimate effect of such adrenergic stimulation is the voiding of gas from the swimbladder system, provided that the communicating

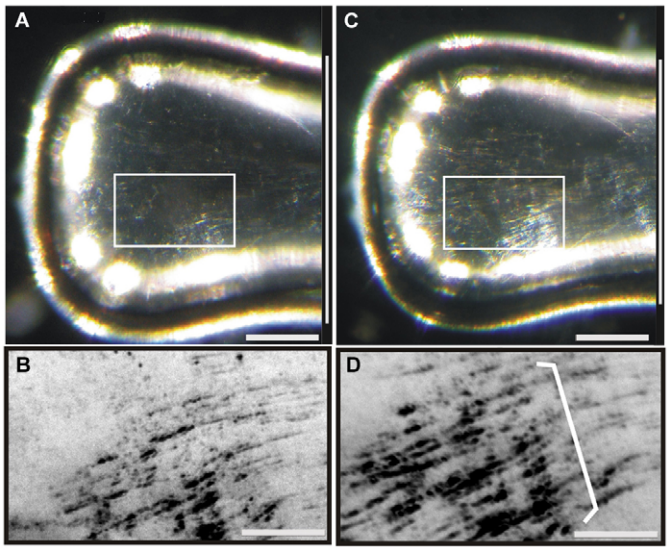

Fig. 6. NA applied to the anterior chamber *in vitro* intensified the folding of connective tissue in the cranioventral region containing the ventral muscle band; folds appear as highly reflective lines under darkfield illumination. Cranial is to the left; anterior–posterior axis is horizontal. (A,B) Before NA exposure, low (A) and high (B) magnification images show a relatively faint pattern of folding (anterior–posterior striations). (C,D) In the same specimen, bath-applied NA (10^{-5} mol l^{-1}, 5 min) caused the fold pattern to be emphasized at both low (C) and high (D, bracket) magnification. Note that the width of the chamber at the right edge of the image in C (indicated by the length of the adjacent vertical line) was less than that in the control (A) as the chamber volume decreased. Greyscale tones were inverted for clarity in panels B and D. Scale bars: 500 μm in A and C; 250 μm in B and D.

duct and the passage from the pneumatic duct into the oesophagus are patent.

The time course of the onset of sympathetically mediated swimbladder deflation in intact zebrafish is not known, but the data presented here suggest that this is likely to occur within a few minutes of an increase in sympathetic drive. Tissue rings isolated from the anterior chamber contracted within seconds of NA application, and in the *in situ* swimbladder gas expulsion began within 1.5 min of NA application. In addition to having a rapid onset, the response of the swimbladder to adrenergic activation was durable; in some *in situ* experiments gas continued to be expelled for up to 0.5 h of NA application. Thus the system that we describe here is effective and appears to be appropriate for modulating buoyancy over the time scale encompassing changes in depth that may occur during mating and feeding behaviours, in response to environmental stressors and perhaps during diurnal changes in depth (Spence et al., 2008).

Adrenergic modulation of the activity of swimbladder components, resulting from reflex increases in sympathetic drive, has been proposed as the major mechanism evoking deflation of this organ in both physoclistous and physostomous teleosts [see reviews by Nilsson (Nilsson, 2009) and others]. For instance, in cod and goldsinny wrass, both physoclists, the diaphragm that separates the gas-secreting from the absorbent region contains smooth muscle and is relaxed by β-adrenergic stimulation (Nilsson, 1971; Fange et al., 1976), thus promoting reabsorption of gas into the bloodstream. In the eel, a physostome in which the pneumatic duct is densely vascularized and serves as a site for gas resorption, β-adrenergic stimulation relaxes the duct wall (Nilsson and Fange, 1967) and causes generalized vasodilatation (Pelster, 1994), also facilitating swimbladder deflation. In the present study we have shown that β-adrenergic stimulation of the smooth muscle in the anterior chamber causes an increase in chamber pressure and the expulsion of gas from the pneumatic duct. The common finding in these widely divergent teleost groups is that, whatever the mechanism, a reduction in swimbladder volume is promoted by the actions of β-receptors, in response to NA released by sympathetic nerve terminals.

In our hands, β-adrenergic stimulation evoked gas release from the swimbladder (see Fig. 3) through direct receptor-mediated actions on smooth muscle (Fig. 2), while α-adrenergic stimulation had no effect on swimbladder volume. This finding is novel, as the usual effect of stimulating β-adrenoreceptors is an inhibition of smooth muscle while α-adrenergic stimulation is usually excitatory. The recent identification of β1-, β2- and β3-adrenergic receptor subtypes in zebrafish tissues (Wang et al., 2009) confirms that such receptors are present in this species, but as these authors did not examine tissue from the swimbladder, anatomical corroboration of our functional results must await further testing.

Smooth muscle in the wall of the posterior chamber lacked any measurable response to adrenergic activation (cf. Fig. 1 and Fig. 2C), a puzzling finding considering the extensive TH-positive innervation of smooth muscle of the lateral muscle band in this chamber (cf. Fig. 7) (Finney et al., 2006) and the fact that smooth muscle in the anterior chamber responded strongly to NA. There may thus be differences in adrenergic receptor complements on smooth muscle in these chambers. It is interesting to note that application of NA to the *in situ* swimbladder preparation caused vasoconstriction in blood vessels of the rete mirabile, mediated largely by α-adrenergic receptors (Dumbarton, 2008). This implies that these vessels are under sympathetic control, operating conventionally through α-adrenergically mediated smooth muscle contraction. Our finding thus confirms a previous report of α-adrenergically mediated vasomotion in the rete of the eel (Pelster, 1994).

It is clear from the discussion above that there is functional adrenergic innervation of both chambers of the zebrafish swimbladder, acting to control anterior chamber volume as well as blood flow in the posterior chamber. However, the mechanism underlying the anomalous β-adrenergic contraction of smooth muscle in the anterior chamber remains to be established.

Muscular organization in the swimbladder

Results from the functional part of this study indicated that the anterior, not the posterior, chamber of the swimbladder played the major role in volume control. The double-chamber morphology of the zebrafish swimbladder is typical of that in nearly all extant cyprinids, and it has been proposed that in this large group of fishes the posterior chamber plays the most important role in adjusting overall swimbladder volume and thus buoyancy [discussed in Fange (Fange, 1966)]. One rationale for this argument has been that the anterior chamber of the swimbladder is connected to the Weberian ossicles and vestibular apparatus so this chamber acts as a resonator in aid of hearing (Evans and Damant, 1929; Fange, 1966). Following that line of reasoning, if this chamber were to be involved in regulating buoyancy as well, it would undergo periodic changes in volume with changes in depth in the water column, a process which could be detrimental to its presumed acoustic function.

We previously reported that the posterior chamber had a well-organized set of largely circumferentially oriented muscles in the lateral muscle band, and proposed that contraction of these muscles

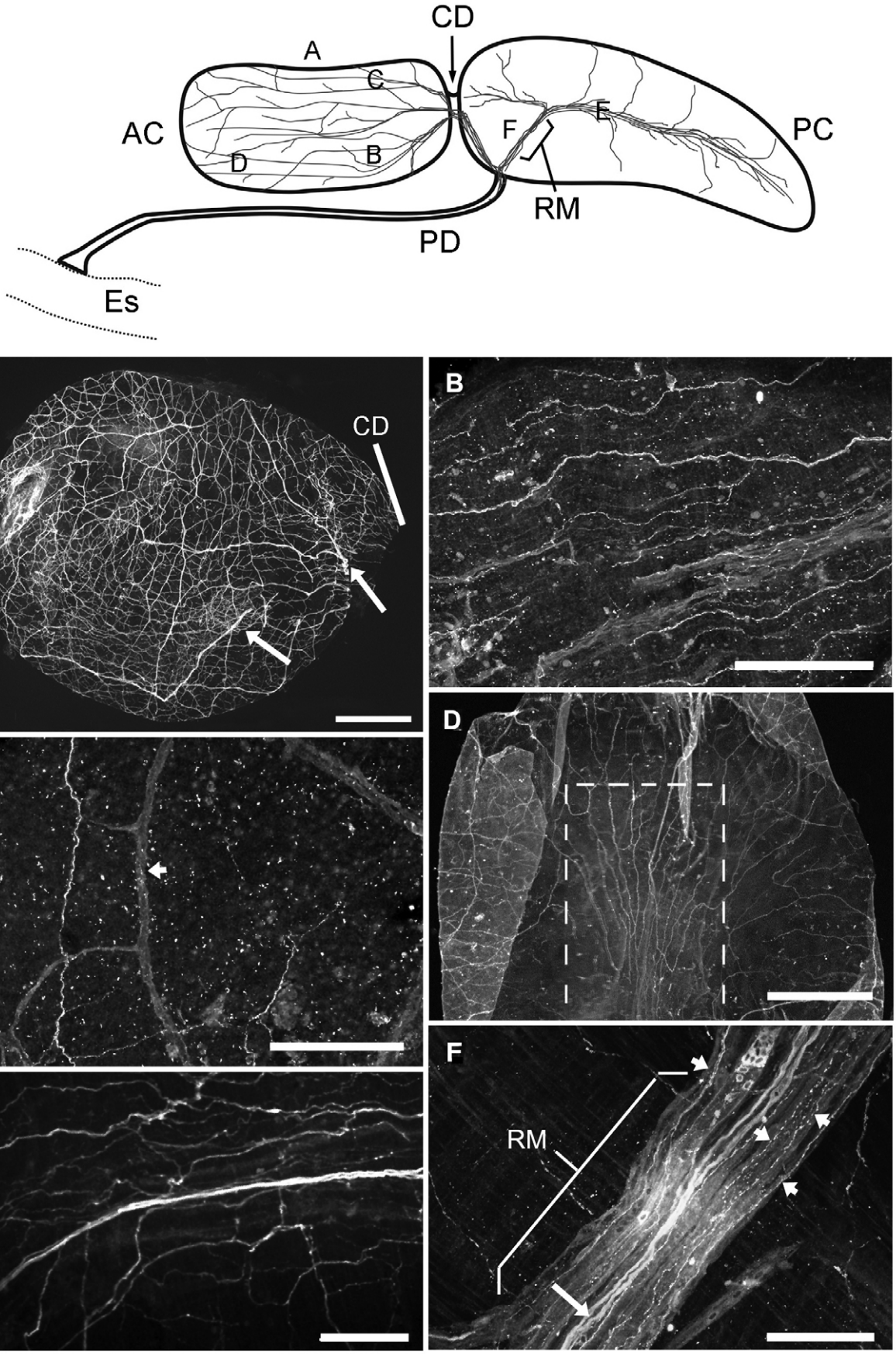

Fig. 7. See next page for legend.

Fig. 7. Details of autonomic innervation in wholemounts of anterior and posterior chamber walls. The schematic diagram illustrates the general swimbladder innervation pattern; letters indicate locations of photomicrographs in panels A–F. (A) In a low-magnification view of the anterior chamber zn-12 immunostaining showed nerve trunks (arrows) and smaller fibres. (B–F) Distribution of neural elements labelled with tyrosine hydroxylase-like immunoreactivity (TH). CD indicates the location of the communicating duct. (B,C) Ventral (B) and dorsal (C) aspects of the anterior chamber wall from the same swimbladder; TH labelling was more dense in the muscular ventral aspect. Note the blood vessel (arrowhead) in C. (D) Low-magnification view of the cranial portion of the ventral anterior chamber showing concentrated ramifications of TH-labelled nerve fibres in the region of the ventral muscle band (dashed line; note image is oriented with the cranial portion uppermost). (E) Detail of TH labelling in the posterior chamber lateral muscle band showing nerve trunk and plexus of single axons ramifying among muscle fibres. (F) Intense TH labelling in nerve (arrow) and single fibres associated with blood vessels of rete mirabile (RM, rete mirabile) on the craniolateral aspect of the posterior chamber. Punctate fluorescence (arrowheads) indicates putative varicosities associated with single fibres. Scale bars: 500 μm in A; 100 μm in B, C and E; 400 μm in D; 200 μm in F.

was probably the major mechanism for emptying the swimbladder to adjust buoyancy (Finney et al., 2006), supporting the concept that the primary role of the anterior chamber was acoustic. In that study we also confirmed earlier reports in other cyprinids (e.g. Evans, 1925) that a ventral muscle band was present in the anterior chamber, but our study did not examine the wall structure of the anterior chamber in detail.

However, the results of the present study strongly indicated the anterior chamber plays an active role in swimbladder deflation. We therefore investigated the detailed structural organization of the musculature and its innervation in this chamber. We have shown that there was a substantial amount of smooth muscle distributed over a large portion of the ventral wall of the anterior chamber, and have further shown that the largely circumferential fibres in this region were organized into what appeared to be bundles that may constitute motor units (Fig. 4). Such an organization has not previously been reported in the swimbladder wall of any teleost, and may in fact be unique to the zebrafish. Furthermore, the pattern of closely packed and highly organized bundles of muscle fibres present in the anterior chamber was not evident in the lateral muscle band of the posterior chamber. Taken together, these anatomical data indicate that the musculature in the anterior chamber is more complex than had previously been suspected; such evidence directly supports our finding that contraction of this musculature reduces swimbladder volume.

A unique feature of the wall of the anterior chamber was the apparent folding of the connective tissue on the lumenal side of the muscle layer (Fig. 4B, Fig. 5). The pattern of these folds ran orthogonal to the main orientation of the circumferential muscle fibres, forming a structure similar to the pleats of an accordion. We further showed that NA application to the anterior chamber significantly accentuated the folding pattern (Fig. 6). The presence of these folds may, therefore, change the mechanical advantage of the system whereby small changes in the length of the muscle fibres could cause larger changes in the effective length of the adjacent chamber wall and thus to the volume of the chamber as a whole.

In contrast, in the posterior chamber there was no strong pattern of folding like that seen in the anterior chamber. This, in conjunction with the observation that neither internal pressure nor volume of the posterior chamber changed during adrenergic stimulation, supports the idea that the anterior chamber plays a major active role in the hydrostatic function of the swimbladder, in addition to the putative role of this chamber in sound reception.

Putative adrenergic innervation in the swimbladder

In this study we confirmed the presence of a large zn-12-immunoreactive nerve trunk coursing to the swimbladder along the pneumatic duct and ramifying in the swimbladder wall to innervate the posterior and anterior chambers. This nerve was first described in the zebrafish by Finney and colleagues (Finney et al., 2006), who proposed that it represented the major source of swimbladder innervation. Here, we have found that in fact only a few TH-positive nerve fibres were present in the nerve accompanying the pneumatic duct; the majority of TH-positive nerve fibres innervating the swimbladder coursed in the smaller nerve along the artery. It is thus likely that the smaller nerve associated with the swimbladder artery described in the present study may comprise the main sympathetic innervation of the zebrafish swimbladder.

Given that the overall density of TH-immunolabelled fibres in the anterior chamber was much lower than that of zn-12-labelled fibres (cf. Fig. 7A and D), the TH-positive axons innervating the anterior chamber represented a subset of the total number of fibres in this chamber. At least some of the non-TH-positive fibres in the anterior chamber are likely to have an afferent rather than an efferent function; apart from a few scattered blood vessels, there are no known effector cells in the dorsal region of the anterior chamber where there is extensive branching of zn-12-immunoreactive fibres. In this context, it is worth noting that Canfield and Eaton (Canfield and Eaton, 1990), among others, proposed that the swimbladder contains receptors sensitive to changes in wall tension that would result from altered swimbladder volume as the animal changed depth.

The finding reported here that TH-immunoreactive nerve fibres were concentrated in the region of the ventral muscle band in the anterior chamber is strongly suggestive of a primary role for this innervation in controlling activity of the smooth muscles in this region, by means of the release of the sympathetic neurotransmitter NA. TH is involved in the synthesis pathway of catecholamines, including NA, in sympathetic nerve terminals, and it is tempting to accept the presence of TH in nerve terminals as *prima facie* evidence of adrenergic, and thus, sympathetic innervation. However, the presence of this enzyme in peripheral nerve fibres does not represent incontrovertible, merely correlative, evidence of sympathetic control. Other studies have shown the presence of NA- as well as TH-containing innervation in teleost swimbladders (Abrahamsson and Nilsson, 1976) (reviewed by Nilsson, 1981; Campbell and McLean, 1994). Yet neither the actual presence of NA in nerve terminals nor its release upon nerve stimulation has been confirmed in the zebrafish swimbladder. Final acceptance of the link between the presence of TH and adrenergic function here must await this confirmation.

CONCLUSIONS

We have shown in this study that the volume of the anterior chamber of the zebrafish swimbladder can be decreased by adrenergically mediated contraction of smooth muscle in the ventral muscle band. Application of NA, acting *via* β-adrenergic receptors on smooth muscle, evoked increases in the force of contraction of wall segments isolated from the anterior chamber, caused an increase in pressure inside this chamber, and evoked contraction of the intact whole anterior chamber which led to gas expulsion from the pneumatic duct and deflation of the swimbladder. The musculature in this band appeared to be highly organized into discrete motor units. Furthermore, the connective tissue substrate of the wall in

this region had apparent folds that may facilitate changes in chamber volume. TH-positive nerve fibres with putative varicosities ramified extensively throughout the ventral muscle band, potentially representing sympathetic terminals. Taken together, these data strongly suggest that deflation of the zebrafish swimbladder is under reflex control by the sympathetic limb of the autonomic nervous system. Our findings in the zebrafish therefore show, for the first time in any physostomous teleost, the effector mechanism that is activated by the deflation reflex to adjust buoyancy in compensating for changes in depth in the water column.

ACKNOWLEDGEMENTS

This research was supported by the Canadian Space Agency under research contract 046016/001/ST awarded to R.P.C. and F.M.S., by National Science and Engineering Research Council Discovery Grants to F.M.S. and R.P.C., and by a Canada Graduate Scholarship awarded to T.C.D. by the Canadian Institutes of Health Research.

REFERENCES

Abrahamsson, T. and Nilsson, S. (1976). Phenylethanolamine-N-methyl transferase (PNMT) activity and catecholamine content in chromaffin tissue and sympathetic neurons in the cod, *Gadus morhua*. *Acta Physiol. Scand.* **96**, 94-99.
Alexander, R. M. (1966). Physical aspects of swimbladder function. *Biol. Rev. Camb. Philos. Soc.* **41**, 141-176.
Alexander, R. M. (1993). Buoyancy. In *The Physiology of Fishes* (ed. D. H. Evans), pp. 75-97. Boca Raton: CRC Press.
Beyer, W. H. (1985). *CRC Handbook of Mathematical Sciences*, 982 pp. Boca Raton: CRC Press.
Briggs, J. P. (2002). The zebrafish: a new model organism for integrative physiology. *Am. J. Physiol. Regul. Integr. Comp. Physiol.* **282**, R3-R9.
Campbell, G. and McLean, J. R. (1994). Lungs and swimbladders. In *Comparative Physiology and Evolution of the Autonomic Nervous System* (ed. S. Nilsson), pp. 157-309. Chur, Switzerland: Harwood Academic Publishers.
Canfield, J. G. and Eaton, R. C. (1990). Swimbladder acoustic pressure transduction initiates Mauthner-mediated escape. *Nature* **347**, 760-762.
Denton, E. J. (1961). The buoyancy of fish and cephalopods. *Prog. Biophys. Biophys. Chem.* **11**, 178-234.
Dumbarton, T. C. (2008). Autonomic control of the swimbladder in the zebrafish (*Danio rerio*). Msc thesis in Department of Physiology and Biophysics, 117 pp. Halifax NS Canada: Dalhousie University.
Edwards, J. G. and Michel, W. C. (2002). Odor-stimulated glutamatergic neurotransmission in the zebrafish olfactory bulb. *J. Comp. Neurol.* **454**, 294-309.
Evans, H. M. (1925). A contribution to the anatomy and physiology of the air-bladder and Weberian ossicles in cyprinidae. *Proc. R. Soc. Lond. B. Biol. Sci.* **97**, 545-576.
Evans, H. M. and Damant, G. C. C. (1929). Observations on the physiology of the swim bladder in cyprinoid fishes. *Brit. J. Exp. Biol.* **6**, 42-55.
Fabbri, E., Capuzzo, A. and Moon, T. W. (1998). The role of circulating catecholamines in the regulation of fish metabolism: an overview. *Comp. Biochem. Physiol. C Pharmacol. Toxicol. Endocrinol.* **120**, 177-192.
Fange, R. (1966). Physiology of the swimbladder. *Physiol. Rev.* **46**, 299-322.
Fange, R. (1983). Gas exchange in fish swim bladder. *Rev. Physiol. Biochem. Pharmacol.* **97**, 111-158.
Fange, R., Holmgren, S. and Nilsson, S. (1976). Autonomic nerve control of the swimbladder of the goldsinny wrasse, *Ctenolabrus rupestris*. *Acta Physiol. Scand.* **97**, 292-303.
Finney, J. L., Robertson, G. N., McGee, C. A., Smith, F. M. and Croll, R. P. (2006). Structure and autonomic innervation of the swim bladder in the zebrafish (*Danio rerio*). *J. Comp. Neurol.* **495**, 587-606.
Giloh, H. and Sedat, J. W. (1982). Fluorescence microscopy: reduced photobleaching of rhodamine and fluorescein protein conjugates by n-propyl gallate. *Science* **217**, 1252-1255.
Harden-Jones, F. R. and Marshall, N. B. (1953). The structure and functions of the teleostean swimbladder. *Biol. Rev.* **28**, 16-83.
McClure, M. M., McIntyre, P. B. and McCune, A. R. (2006). Notes on the natural diet and habitat of eight danionin fishes, including the zebrafish *Danio rerio*. *J. Fish. Biol.* **69**, 553-570.
Miklósi, A. and Andrew, R. J. (2006). The zebrafish as a model for behavioral studies. *Zebrafish* **3**, 227-234.
Nemtsas, P., Wettwer, E., Christ, T., Weidinger, G. and Ravens, U. (2010). Adult zebrafish heart as a model for human heart? An electrophysiological study. *J. Mol. Cell. Cardiol.* **48**, 161-171.
Nilsson, S. (1971). Adrenergic innervation and drug responses of the oval sphincter in the swimbladder of the cod (*Gadus morhua*). *Acta Physiol. Scand.* **83**, 446-453.
Nilsson, S. (1972). Autonomic vasomotor innervation in the gas gland of the swimbladder of a teleost (*Gadus morhua*). *Comp. Gen. Pharmacol.* **3**, 371-375.
Nilsson, S. (1981). On the adrenergic system of ganoid fish: the Florida spotted gar, *Lepisosteus platyrhincus* (Holostei). *Acta Physiol. Scand.* **111**, 447-454.
Nilsson, S. (1983). *Autonomic Nerve Function in the Vertebrates*. Berlin: Springer-Verlag.
Nilsson, S. (2009). Nervous control of fish swimbladders. *Acta Histochem.* **111**, 176-184.
Nilsson, S. and Fange, R. (1967). Adrenergic receptors in the swimbladder and gut of a teleost (*Anguilla anguilla*). *Comp. Biochem. Physiol. A* **23**, 661-664.
Pelster, B. (1994). Adrenergic control of swimbladder perfusion in the European eel *Anguilla anguilla*. *J. Exp. Biol.* **189**, 237-250.
Pelster, B. (1997). Buoyancy at depth. In *Fish Physiology*, vol. 16 (ed. D. J. Randall and A. P. Farrell), pp. 195-237. San Diego: Academic Press.
Pelster, B. (2009). Buoyancy control in aquatic vertebrates. In *Cardio-Respiratory Control in Vertebrates: Comparative and Evolutionary Aspects* (ed. M. L. Glass and S. C. Wood). Berlin, Heidelberg: Springer.
Robertson, G. N., Lindsey, B. W., Dumbarton, T. C., Croll, R. P. and Smith, F. M. (2008). The contribution of the swimbladder to buoyancy in the adult zebrafish (*Danio rerio*): a morphometric analysis. *J. Morphol.* **269**, 666-673.
Scheid, P., Pelster, B. and Kobayashi, H. (1990). Gas exchange in the fish swimbladder. *Adv. Exp. Med. Biol.* **277**, 735-742.
Small, J., Rottner, K., Hahne, P. and Anderson, K. I. (1999). Visualising the actin cytoskeleton. *Microsc. Res Tech.* **47**, 3-17.
Smit, G. L., Hattingh, J. and Burger, A. P. (1979). Haematological assessment of the effects of the anaesthetic MS 222 in natural and neutralized form in three freshwater fish species: interspecies differences. *J. Fish. Biol.* **15**, 633-643.
Spence, R., Gerlach, G., Lawrence, C. and Smith, C. (2008). The behaviour and ecology of the zebrafish, *Danio rerio*. *Biol. Rev. Camb. Philos. Soc.* **83**, 13-34.
Sun, X. and Ng, Y. C. (1998). Effects of norepinephrine on expression of IGF-1/IGF-1R and SERCA2 in rat heart. *Cardiovasc. Res.* **37**, 202-209.
Trevarrow, B., Marks, D. L. and Kimmel, C. B. (1990). Organization of hindbrain segments in the zebrafish embryo. *Neuron* **4**, 669-679.
Wang, Z., Nishimura, Y., Shimada, Y., Umemoto, N., Hirano, M., Zang, L., Oka, T., Sakamoto, C., Kuroyanagi, J. and Tanaka, T. (2009). Zebrafish beta-adrenergic receptor mRNA expression and control of pigmentation. *Gene* **446**, 18-27.
Webber, D. M., Aitken, J. P. and O'Dor, R. K. (2000). Costs of locomotion and vertical dynamics of cephalopods and fish. *Physiol. Biochem. Zool.* **73**, 651-662.
Westerfield, M. (2007). *The Zebrafish Book: A Guide for the Laboratory Use of Zebrafish* (*Danio rerio*). Eugene, OR: University of Oregon Press.